ELSEVIER

Catalysis Today 70 (2001) 43–58

CATALYSIS TODAY

www.elsevier.com/locate/cattod

On the critical use of molar absorption coefficients for adsorbed species: the methanol/silica system

Claudio Morterra [a,*], Giuliana Magnacca [a], Vera Bolis [b]

[a] *Department of Chemistry IFM, University of Turin, Via P. Giuria 7, 10125 Turin, Italy*
[b] *University of Eastern Piedmont "Amedeo Avogadro", DISCAFF, Viale Ferrucci 33, 28100 Novara, Italy*

Abstract

The ambient temperature adsorption of methanol vapour on two preparations of non-porous silica (Aerosil 50 and Aerosil 300) activated at two different temperatures (∼300 and 1073 K) has been studied by gas-volumetric and in situ transmission FTIR spectroscopic methods, in order to check the validity of equations of the Beer–Lambert type in the case of heterogeneous systems. The results indicate that, for both physically adsorbed and chemisorbed methanol, the calculated integral molar absorption coefficients are of the right order of magnitude (as compared with those typical of methanol in homogeneous phase), but the actual values vary much from one sample to another, depending on several factors. Among the factors, very important turn out to be: the specific surface area of the adsorbent, the sample thickness, the surface dehydration level of the adsorbing system and, most probably, the scattering properties of the adsorbent. In particular, the first two factors of variability imply that, when dealing with the spectral response of adsorbed species, an adequate normalization of the observed band intensities against sample surface area as well as against sample weight is difficult to achieve. The conclusion is that: (i) in the case of either physically adsorbed or chemisorbed species, the concept of molar absorption coefficient is virtually impossible to apply in general terms; (ii) the values calculated as "apparent" absorption coefficients cannot be transferred from one system to another, even if the ε figures calculated for adsorbed species do fall in the range of ε values determined for homogeneous systems.

Keywords: IR absorption coefficients; Methanol; Adsorption; Aerosil

1. Introduction

IR spectroscopy applied to surface phenomena started with few pioneering works in the late 1950s, grew fast, and in little over 40 years that technique has brought us a great deal of understanding of chemical and/or structural aspects of both surface functionalities (i.e., chemical species present at the surface of solid systems) and molecular species adsorbed thereon. The number of surface species identified by in situ IR spectroscopy is virtually countless, as equally countless are the transformations undergone by surface species upon physical and/or chemical treatments that have been postulated on the basis of their vibrational behaviour.

The major drawback of IR spectroscopy applied to surface species consists in the fact that, being eminently qualitative in nature, very seldom does the technique bring any information also on the quantitative aspects of surface phenomena. The quantitative comprehension of surface processes, possibly identified by in situ IR spectroscopy, must be therefore obtained by means of other independent analytical techniques like, for instance, microgravimetric or gas-volumetric ones.

* Corresponding author. Tel.: +39-11-670-7589; fax: +39-11-670-7855.
E-mail address: morterra@ch.unito.it (C. Morterra).

0920-5861/01/$ – see front matter
PII: S0920-5861(01)00406-0

More ambitiously, one could try to give in situ IR spectroscopic measurements a more immediate quantitative meaning by directly combining them with proper analytical determinations, carried out in strictly corresponding conditions. This conclusion is not so obvious as it may look at first sight: in fact, it implies that, in the whole course of the experiments being investigated, spectroscopic and analytical data yield strictly corresponding information. In other words, this conclusion implies that for surface species, that were formed in a heterogeneous system, relations of the type of the Beer–Lambert (B–L) equation, reported in (1), hold in all conditions explored, even if it is known that the B–L equation was proposed and verified only for homogeneous systems:

$$A_\nu = \varepsilon_\nu C d \tag{1}$$

where A_ν is the integral absorbance over a wavenumber interval ν (cm^{-1}), C the concentration of the absorbing species ($mol\,l^{-1}$), d the optical path (cm), and ε_ν the integral molar absorption coefficient ($mol^{-1}\,l\,cm^{-2}$) or ($mol^{-1}\,cm \times 10^3$).

Trying to apply an equation of the B–L type to a surface species, absorbing in a wavenumber interval designated by the Greek letter ν and yielding, in the ith condition examined, the integral absorbance $(A_\nu)_i$, if a parallel analytical determination indicates $(n_w)_i$ moles of that species to be present per unit sample weight, we can write

$$(A_\nu)_i = \varepsilon_\nu (n_w)_i \frac{w}{Sd} d \tag{2}$$

where w is the weight of the adsorbing sample (g), S the geometric area of the sample (cm^2), and d the geometric thickness of the sample (cm).

Here, we have been obliged to introduce a first conceptual approximation: although it is known that adsorption is a heterogeneous phenomenon that occurs, on each particle constituting the sample, at the bi-dimensional interphase conventionally termed the Gibbs surface [1], the $mol\,cm^{-3}$ concentration of adsorbed species has been expressed in the hypothesis of a homogeneous distribution of the adspecies within the geometric volume of the solid sample.

A second approximation follows: we are now obliged to eliminate the two d terms from Eq. (2), yielding the following equation:

$$(A_\nu)_i = \varepsilon_\nu (n_w)_i \frac{w}{S} \tag{3}$$

even if we know that the two thickness terms are not equivalent, one (denominator) being a geometrical one, relatively easy to determine, and the other one (numerator) being an optical path that, in the case of powdery and scattering solid materials, is certainly not coincident with the geometric thickness and is virtually impossible to evaluate.

Expressing now the adsorbed amounts deriving from an analytical determination in the more usual n_S form (moles adsorbed per unit surface area ($mol\,m^{-2}$)), Eq. (3) rearranges as follows:

$$\frac{(A_\nu)_i}{w A_S} S = \varepsilon_\nu \frac{(n_w)_i}{A_S} \tag{4}$$

where A_S is the specific surface area of the adsorbing material ($m^2\,g^{-1}$) or, more concisely, as given below

$$(A^*_\nu)_i = \varepsilon_\nu (n_S)_i \tag{5}$$

where $(A^*_\nu)_i$ (cm^{-1}) is the integral absorbance, normalized against the sample surface area (A_S) and against the sample surface density (w/S).

The apparent integral molar absorption coefficient of the adsorbed species, deriving from the ith determination, turns out to be

$$\varepsilon_\nu = \frac{(A^*_\nu)_i}{(n_S)_i} \tag{6}$$

and its units are $mol^{-1}\,cm$.

Some of the conceptual limits of applicability of equations of the B–L type to heterogeneous systems were proposed some years ago [2], as also stressed was the critical use of concepts like that of molar absorption coefficient when applied to adsorbed species. Still, in that particular case (concerned with the room temperature adsorption of carbon monoxide at the surface of some TiO_2-based systems) as well as in several other similar cases considered afterwards (all dealing with the weak adsorption of CO, yielding localized interactions and low coverages; e.g., see Refs. [3–5,33,34]), the absorption coefficients obtained through the combined use of in situ transmission IR spectra and gas-volumetric determinations turned out to be quite consistent and reasonably well

reproducible. It could be thus concluded that at least in the case of weak adsorption processes of the Lewis acid–base type, and leading to low surface coverages, equations of the type reported in (4) and (5) are reasonably accurate, in spite of the approximations introduced.

Also other cases have been examined. Starting with the early work by Hughes and White [6], dealing with the adsorption of the strong base pyridine on insulating oxidic systems, the assumption of the validity of equations of the B–L type for heterogeneous systems has been invoked several times also in the case of strong localized adsorptions of the acid–base type (e.g., see Refs. [7–9]). Moreover, the molar absorption coefficients calculated for a strong adsorbate like pyridine have been claimed to possess virtually constant values on different oxidic systems [8], and thus to be transferable from one system to another, though of the same chemical/physical type. This conclusion, very convenient in terms of practical applications, is far more surprising than the previous one, and its limits of validity are presently being checked by the uptake of strong adsorbates at the surface of different preparations of otherwise strictly equivalent adsorbing systems.

Aim of the present contribution is to bring some experimental evidence of cases in which IR spectral intensities and quantitative analytical data do not match, so that the application of equations like those reported in (4) and (5) is inadequate, even in approximate terms. The solid/gas heterogeneous system to be dealt with here, the adsorption of methanol on silica, has been chosen for the following reasons: (i) the adsorption mechanism involved is rather complex, and chemically quite different from the acid/base mechanisms mentioned above. In fact, in some cases there is a strong and localized chemisorption process, whereas in all cases there is a weak and non-localized physisorption process. In particular, the physical adsorption process, based on the formation of multiple H-bondings, is quite weak in energetic terms, and thus somehow comparable to the adsorption of CO on d^0 oxidic systems, but unlike that it involves the whole surface and leads to the creation of a non-localized multilayer uptake (as typical of physisorption phenomena); (ii) the complex CH_3OH/SiO_2 system has been long investigated in most of its qualitative and theoretical aspects, so that only some quantitative aspects of the description of this system need to be taken into account.

2. Experimental

2.1. Materials and samples preparation

In the present contribution, that is part of a wider investigation devoted to the study of some surface properties of many types of SiO_2-based systems, only two fairly different preparations of non-porous fumed SiO_2 of the Aerosil (Degussa) family, termed A_{50} and A_{300}, respectively, will be considered in detail. Occasionally, a third system of the same type, termed A_{200}, will be considered for mere comparison purposes. A_{50} and A_{300} are characterized by quite different surface area (50, and 296 $m^2\,g^{-1}$, respectively), and rather different morphological features, as shown by the electron micrographs reported in Fig. 1. The A_{50} system is made up of large, well separated, and highly regular (i.e., quasi-spherical) particles of some 60 nm diameter, whereas the A_{300} system is made up of definitely smaller particles (average diameter: 10–15 nm) of far less regular shape. Consistent with the different average particles size, also the light-scattering features of the two silica preparations are expected to be quite different. Fig. 2 reports the transmittance vs. wavelength spectral profile of A_{50} and A_{300} and shows that after the top transmittance region (centred at $\sim$2100 cm^{-1}), the light scattering losses of the former larger-particles material are quite severe (see curve b, relative to a very thin sample of A_{50}), whereas in the case of the latter material, characterized by much smaller particles, the scattering-loss profile is almost flat (see curve a of Fig. 2, relative to a very thin sample of A_{300}).

Before methanol adsorption, and for *both* spectroscopic and gas-volumetric experiments (in order to avoid side-effects due to samples texture on adsorptive properties), silica specimens were prepared in the form of self-supporting pellets by compaction under a constant pressure of 4 tons, and then were activated in vacuo (residual pressure $<10^{-5}$ Torr) at the chosen temperatures for $\sim$4 h. Out of the many activation conditions adopted, only two activation temperatures will be considered here for the two materials: nominal ambient temperature ($\sim$300 K), and 1073 K; the two activation temperatures chosen are important in that they represent fairly different stages of the thermal surface dehydration process. The corresponding specimens are designated in the text and figures by the

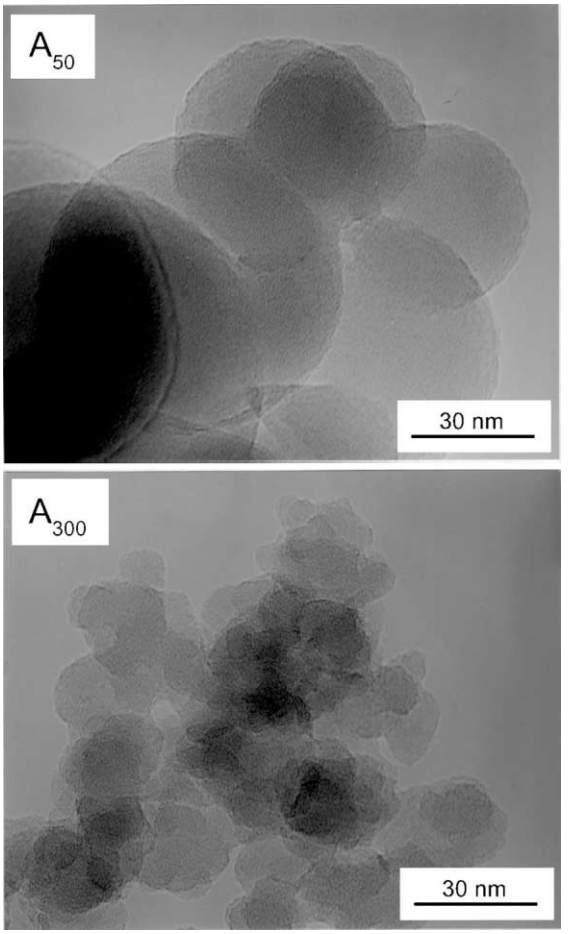

Fig. 1. Transmission electron microscopy images of the amorphous non-porous Aerosil preparations A_{50} (upper part) and A_{300} (lower part).

symbols A_S300 and A_S1073, respectively (where the subscript *S* stands for 50 and 300, respectively, and only occasionally for 200, as reported in the text).

2.2. Gas-volumetric isotherms

Quantitative adsorption measurements were carried out at 303 K in a gas-volumetric apparatus connected with a heat-flow microcalorimeter (Tian Calvet type), as described elsewhere [10]. Adsorption heats were also determined, but are not discussed here as they are not pertinent to the present work. With each sample, a methanol adsorption run was first carried out up to an equilibrium pressure of some 70 Torr (the *primary adsorption*). Then, after a long contact (∼6 h) with the highest methanol pressure reached, the system was thoroughly evacuated at the same temperature (303 K) for at least 5 h, and subsequently a second methanol adsorption run, up to the same final pressure, was carried out (the *secondary adsorption*). The difference between the two adsorption runs (if any), is related to the fraction of adsorbate that remains irreversibly held on the silica surface at the adsorption/desorption temperature.

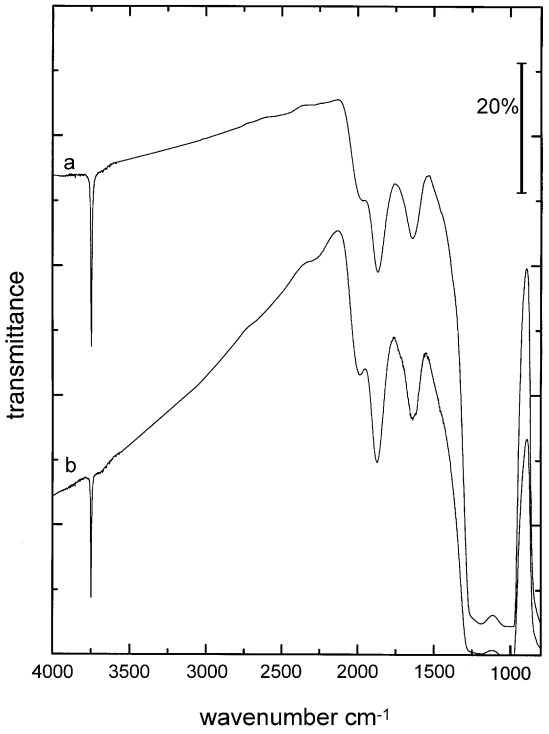

Fig. 2. Whole-range FTIR transmittance spectra of amorphous non-porous Aerosil specimens: (a) $A_{300}1073$, thin sample (6.5 mg cm^{-2}); (b) $A_{50}1073$, thin sample (7.0 mg cm^{-2}).

2.3. IR spectroscopic adsorption experiments

For IR experiments, “thin” samples (surface density of the order of ∼6−7 mg cm^{-2}) and “thick” samples (surface density of the order of ∼35–40 mg cm^{-2}) were prepared, following the procedure reported above. Methanol uptake was carried out on all samples in conventional quartz cells equipped with KBr IR windows and suitable for in situ activation and

adsorption experiments, connected with a conventional high vacuum apparatus. FTIR spectra were recorded in the transmission/absorption mode at a resolution of 2 cm^{-1} with a Bruker spectrophotometer 113v, equipped with MCT detector. In the spectroscopic adsorption experiments, the first methanol adsorption run (primary adsorption) was followed by a prolonged contact in the IR measurement cell with the highest methanol pressure reached, and then by a prolonged evacuation at the adsorption temperature. In view of the strictly in situ procedure adopted, the fraction of adsorbate that remains irreversibly held on the silica surface at the adsorption/desorption temperature is thus represented by the IR spectrum obtained after the long evacuation step. As for the spectroscopic equivalent of the secondary adsorption run of the gas-volumetric experiments, it could be either obtained by actually carrying out a second in situ adsorption run (the optical secondary adsorption), or possibly simulated by interactive spectral subtraction from the spectra of the primary adsorption run of the contributions due to the irreversibly held adsorbate.

2.4. Electron microscopy

Transmission electron microscopy (high resolution) images were obtained with a Jeol JEM 2000 EX apparatus (200 kV acceleration), equipped with a top-entry stage. Silica powder samples for TEM analysis were deposited from isopropanol dispersions on Cu grids, coated with a "holey-carbon" film.

3. Results and discussion

3.1. The adsorption of methanol on silica

The CH_3OH/SiO_2 system, as well as other related systems, have been extensively studied by several authors (just to mention a few, see Refs. [11–22]), and most of the relevant spectroscopic, theoretical and microcalorimetric aspects have been considered in detail.

The major phenomena taking place in the ambient temperature CH_3OH/SiO_2 system can be briefly summarized as follows:

1. On silica-based materials activated at $T_{act} \leq 623$ K, all methanol is adsorbed in an undissociated molecular form, through the formation of a complex system of H-bonding interactions: the surface OH functionalities of silica are thought to be the initial adsorbing sites, from which the formation of tri-dimensional polymeric methanol chains starts. The physically adsorbed methanol phase is characterized by a complex IR absorption in the C–H stretching region (ν_{CH}), three main components being observed at $\sim$3000 cm^{-1} [$\nu'_{as}(CH_3)$], 2950 cm^{-1} [$\nu''_{as}(CH_3)$], and 2845 cm^{-1} [$\nu_s(CH_3)$], respectively. A typical spectrum observed in the ν_{CH} region for physisorbed methanol is shown in the top spectral set of Fig. 3A, curves b (i.e., the spectrum "as is") and c (the same spectrum, after background subtraction and linearization).

   The vast majority of the multi-layer molecularly adsorbed methanol phase has been reported by several authors to be reversible upon evacuation at ambient temperature, whereas a variable minor fraction may remain adsorbed at ambient temperature (it will desorb at a temperature of some 423 K) due to the formation of 2–3 H-bondings of medium–low strength per methanol molecule [11,12,19,22].
2. On silica-based materials activated at $T_{act} > 623$ K, the formation of a tri-dimensional physisorbed methanol phase is still the far dominant effect, especially at medium–high methanol coverages. But, starting from the earliest stages of the adsorption process (i.e., at low methanol coverages), also a much slower dissociative chemisorption process starts occurring at surface defective sites. These sites, that are supposed to be edge-shared tetrahedral defects [23–25] and/or strained siloxane bridges [11,12,26], were produced at the surface of the covalent silica network during the medium–high temperature activation step. The dissociative chemisorption process leads to the formation of surface hydroxyls and surface methoxy groups, according to the reaction path schematically presented in Scheme 1. [1]

The newly formed O–CH_3 groups are quite stable (in fact, their thermal elimination only begins at some 873 K), and in the C–H stretching region they

[1] The asterisk on the oxygen atom indicates that the reactive surface defect is actually represented by a surface Si–O–Si bridge of unusual size and/or geometry [20].

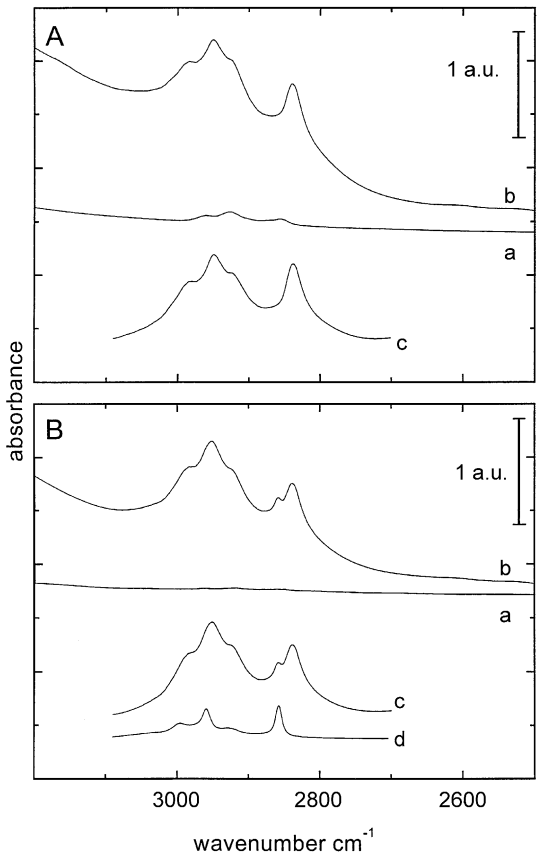

Fig. 3. Absorbance spectra in the CH_3 stretching region, relative to a thin $A_{300}300$ sample (A) and a thin $A_{300}1073$ sample (B). The spectral segments correspond, in each part and when present, to the following: (a) background; (b) primary methanol adsorption run, after long contact with 70 Torr methanol (70 Torr is the highest adsorptive pressure reached); (c) as for spectrum b, after background subtraction (i.e., b − a), and liberation from the contribution of all other superimposed absorptions (e.g., the band of H-bonded OH species); (d) as for spectrum c, after prolonged evacuation at ambient temperature of the reversible (i.e., physisorbed) methanol fraction.

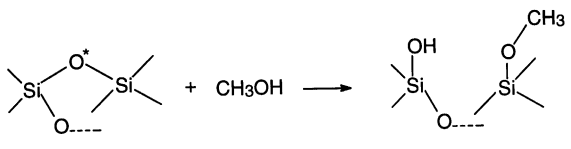

Scheme 1.

are characterized by typical spectral components at 3000 cm^{-1} [$\nu'_{as}(CH_3)$], 2958 cm^{-1} [$\nu''_{as}(CH_3)$], and 2858 cm^{-1} [$\nu_s(CH_3)$], respectively. The latter vibrational mode is the one that makes the presence of a chemisorbed methanol phase most evident, also in the presence of an excess of physisorbed methanol [20]. Typical ν_{CH} spectra are shown in the bottom spectral set of Fig. 3B: curve b is the ν_{CH} spectrum "as is", after long contact with the highest methanol pressure reached, and is thus relative to the simultaneous presence of both physisorbed and chemisorbed methanol, curve c is the same spectrum of curve b, after background subtraction and linearization, whereas curve d is the ν_{CH} spectrum of the fraction that remains adsorbed after prolonged evacuation at ambient temperature (i.e., it represents the chemisorbed methanol phase).

3.2. Gas-volumetric adsorption isotherms

Apart from a previous comparative study on amorphous and crystalline silicas [27,35], to the best of our knowledge the adsorption of methanol on different types of amorphous silica treated at different temperatures has never been considered so far in quantitative terms.

Fig. 4 reports, for the two silica specimens examined in detail in this work and for both activation conditions considered, the secondary methanol adsorption isotherms (dark symbols) expressed in terms of n_S (moles adsorbed per unit surface area) vs. methanol equilibrium pressure (Torr). Only for one specimen ($A_{300}T$), Fig. 4B reports, as an example, also the primary adsorption isotherms (open symbols), from which it is deduced that: (i) on the samples activated at low temperature, the amount of molecularly (i.e., undissociated) adsorbed methanol that remains adsorbed after a prolonged evacuation at ambient temperature (see in Fig. 4B, the difference between curves I and II for $T_{act} = 300$ K) is negligible with respect to the reversible fraction of the physisorbed methanol phase. The fact that this non-reversible fraction of the physisorbed phase will not be considered in the following, using for both volumetric and spectroscopic experiments the plain secondary isotherms, should thus cause an error that is negligible in quantitative terms and, in any event, is equivalent for the two families of isotherms; (ii)

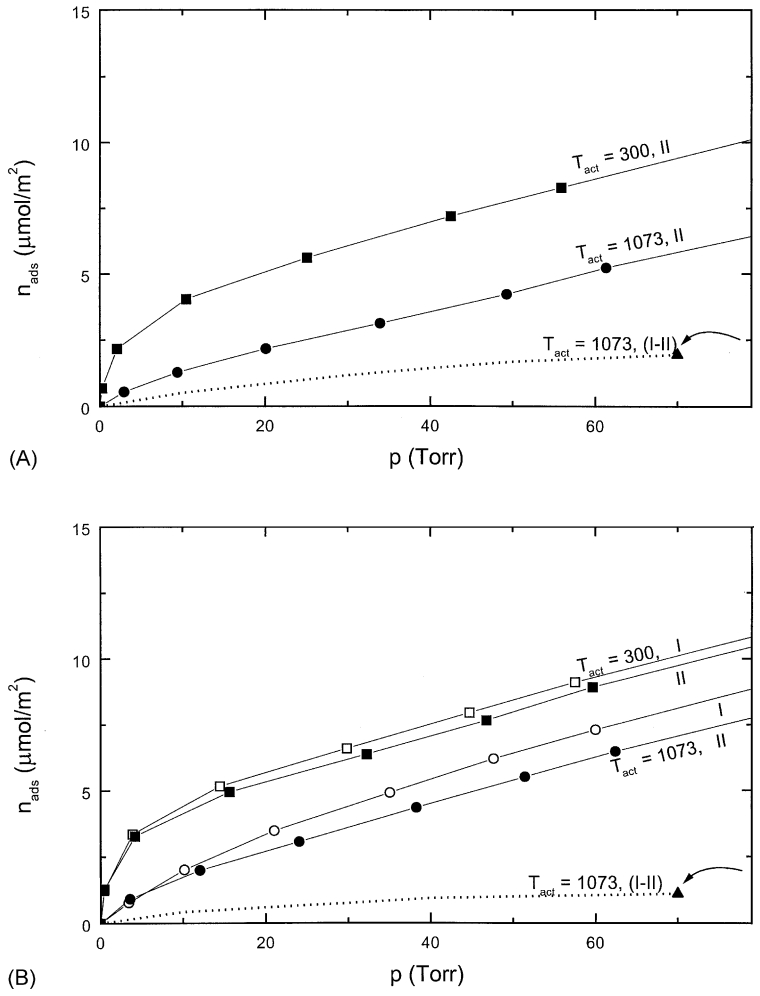

Fig. 4. Normalized volumetric adsorption isotherms (μmol m^{-2} vs. Torr) of methanol adsorbed at 303 K on Aerosil $A_{50}T$ (A) and on Aerosil $A_{300}T$ (B). The temperatures of sample activation (K) are reported on the curves. The symbols I and II stand for primary and secondary adsorption run, respectively. The lower-lying dotted curves, marked (I − II), correspond to the irreversibly adsorbed (chemisorbed) methanol phase, as obtained by the difference between primary and secondary adsorption run. The last chemisorption point on each (I − II) curve, located at $p = 70$ Torr and indicated by an arrow, represents the saturation of methanol chemisorptive capacity of each sample activated at high temperature.

the amount of chemisorbed (dissociated) methanol that forms on samples activated at high temperature is quite appreciable (see in Fig. 4A and B, the low-laying curves marked $T_{act} = 1073$ K (I − II) and, in part B, the actual difference between the primary adsorption curve (I) and the secondary one (II) in the curves set marked $T_{act} = 1073$, relative to the system A_{300}). After prolonged contact, the chemisorbed fraction may amount to some 0.9–1.2 μmol m^{-2}, and its accurate elimination from both volumetric and spectroscopic adsorption data is vital when quantitative information on the physisorbed methanol phase is sought for.

The present quantitative data are consistent with some of the very few quantitative data reported in the literature (e.g., see Ref. [28]: a similar high-area Aerosil (A_{200} activated at low temperature) was used there, and our $A_{300}300$ system presents an overall uptake that is somewhat lower by less than 10%).

Comparison of the volumetric isotherms reported in Fig. 4 indicates that:

1. The normalized amounts of methanol adsorbed by H-bonding on the two Aerosil samples activated at ambient temperature turn out to be (almost) perfectly coincident in the whole pressure range explored. This means that, in spite of the different surface area and morphology of the two samples, to an equivalent starting condition of nominally complete surface hydration, does indeed correspond a virtually equivalent adsorbing capacity, i.e., an equivalent surface concentration of adsorbing sites. On samples still so highly hydrated, the adsorbing sites are thought to be a complex ensemble of "free" isolated OH groups (meaning, free from H-bonding), free geminal OH groups, and clusters of interacting OH groups, mutually perturbed by H-bonding. On highly hydrated specimens like A_S300, the first family of OH species is expected to be far less abundant than the other two, whereas the last family is expected to be the most abundant one. It is probably for this reason that fairly different specimens, isolated in the same high hydration stage, tend to behave in an almost indistinguishable way.

   A first question to be answered, when dealing with the IR spectroscopic description of methanol adsorption, will be: do IR spectra confirm that methanol uptake is the same on different highly hydrated Aerosil preparations?
2. The activation at high temperature causes a drastic decrease of the adsorbing capacity of all samples, the decrease being definitely more abundant for the low-area A_{50} preparation. (For instance, at 10 Torr, the reduction of reversible methanol uptake is to ∼30% for A_{50} and only to ∼45% for A_{300}, whereas at 50 Torr the reduction is to ∼55% for A_{50} and to ∼70% for A_{300}.) Since for thermal activation at temperatures as high as 1200 K neither morphological nor surface area changes are expected to occur yet on non-porous Aerosil systems, the observed decrease of physisorbed uptake must be ascribed solely due to the consequences of the surface dehydroxylation process, i.e., to a drastic decrease of the surface concentration of OH sites from where the construction of tri-dimensional methanol polymeric chains starts. It is also deduced that the large-particles and low-area A_{50} system dehydrates more promptly than do small particles and high-area systems like A_{300}. This is confirmed by a definitely larger normalized amount of irreversibly adsorbed (chemisorbed) methanol observed in the case of $A_{50}1073$ (curve marked $T_{act} = 1073$ (I − II) in Fig. 4A) than in the case of $A_{300}1073$ (curve marked $T_{act} = 1073$ (I − II) in Fig. 4B).

   A second type of question to be answered, when dealing with the IR spectroscopic description of methanol adsorption, will be: do IR spectra confirm the decrease of methanol physisorption capacity with increasing activation temperature, and the different extent of such decrease on different Aerosil preparations? Also: do IR spectra confirm the decrease of methanol chemisorption capacity on passing from low-area to high-area Aerosil preparations treated in the same medium–high temperature conditions?

3.3. IR spectral patterns and optical adsorption isotherms

Selected examples of spectral patterns relative to some primary and secondary methanol adsorption runs are presented in Fig. 5, where part A is relative to the system A_{50}, and part B to the system A_{300}. The curve sets a–c concern thin samples of both specimens, whereas the curve sets d concern thick samples of both specimens, as explained in the legends. The spectral patterns show many detailed aspects of the complex adsorption process: as expected, in situ IR spectra turn out to be far more suitable than adsorption isotherms for the comprehension in qualitative terms and at a molecular level of the various phases of the adsorption phenomenon. Still, most of the spectroscopic aspects of methanol adsorption at ambient temperature on silica-based systems have already been described in great detail (e.g., see Ref. [20], and references therein), and since we are here mostly interested in the possibility of evaluating the methanol adsorption process in quantitative terms, very little discussion will be dedicated to the spectral patterns of Fig. 5.

In particular, the following spectroscopic aspects deserve some comment:

1. On the preparation of A_{300} (Fig. 5B), for which also the primary adsorption pattern after activation at high temperature ($T_{act} = 1073$) is reported,

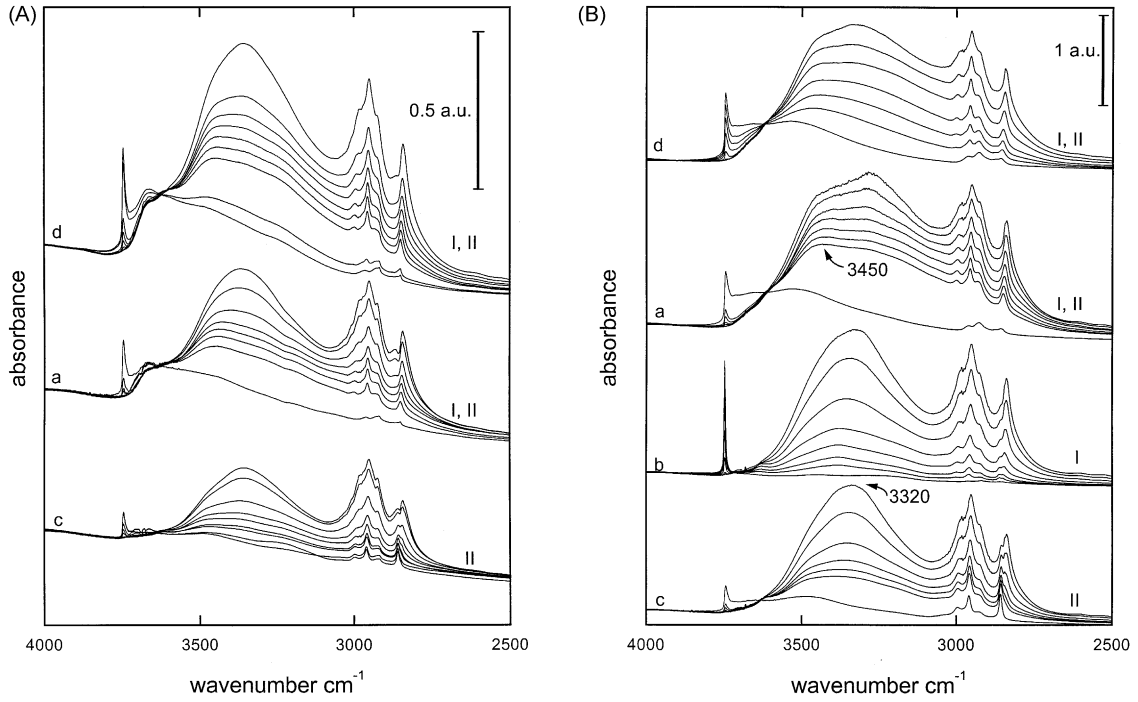

Fig. 5. FTIR absorbance spectral patterns, in the 4000–2500 cm^{-1} range (OH and OCH_3 stretching vibrations), relative to the adsorption of methanol at −300 K on Aerosil preparations $A_{50}T$ (A) and $A_{300}T$ (B). Adsorptive pressures in the range 0–70 Torr. The patterns correspond, in each section and when present, to the following specimens: (a) thin sample, activated at 300 K, primary adsorption run (virtually coincident with the secondary one); (b) thin sample, activated at 1073 K, primary adsorption run; (c) thin sample, activated at 1073 K, secondary adsorption run; (d) thick sample, activated at 300 K, primary adsorption run (virtually coincident with the secondary one).

the decrease of sites concentration made available for methanol physisorption on passing from low-temperature activation (300 K; see the lowest-laying spectrum in the spectral set a) to high-temperature activation (1073 K; see the lowest-laying spectrum in the spectral set b) is clearly monitored in the ν_{OH} spectral region: there is a net increase and sharpening of the band at ∼3747 cm^{-1} (due to the increasing surface concentration of isolated free OH species, and to the decreasing concentration of free geminal OH species), while there is the disappearance of a complex absorption extending from ∼3730 to ∼3100 cm^{-1} (due to the complete elimination of the clusters of surface OH groups interacting by H-bonding). This modification of the spectral profile, brought about by the thermal activation process, is perfectly understandable in spectroscopic terms, although it is virtually impossible to give it a quantitative meaning. From other independent data, reported in the literature (e.g., see Refs. [11,12,29,30]), it is known that upon activating in vacuo amorphous non-porous silica, the average surface OH population changes a lot, and passes from over 8 groups nm^{-2} at ambient temperature, to ∼3.5 groups nm^{-2} at 623 K, and to less than ∼1.2 groups nm^{-2} at 1073 K.

The background spectral profile of the secondary adsorption pattern (see the lowest-lying spectrum in the spectral set c of Fig. 5B) is quite different from that of the primary one, as the slow methanol chemisorption process (accomplished during the primary adsorption run and during the long contact with the highest methanol pressure reached) brought about the formation of stable surface methoxy groups and of an equivalent number of surface OH groups, that are either of the geminal type or of the H-bonding interacting type. The decreased secondary physisorption capacity

of $A_{300}1073$ (set c) with respect to $A_{300}300$ (set a) is thus simply suggested by a decreased overall intensity in the whole ν_{OH} stretching region (3800–3100 cm^{-1}).

2. On $A_{50}T$ (Fig. 5A), a significant decrease of secondary methanol adsorption capacity on passing from the sample activated at low temperature to the sample activated at high temperature is immediately suggested by an overall decrease of all spectral intensities produced during the secondary methanol adsorption run (compare the spectral sets a and c in Fig. 5A), even if the decrease is definitely more evident in the ν_{OH} region than in the ν_{CH} one. But on $A_{300}T$ (Fig. 5B), no appreciable decrease at all is noted in the ν_{CH} region during secondary methanol uptake on the sample treated at high temperature (see the spectral sets a and c in Fig. 5B), whereas (only) a net decrease of the bandwidth in the broad absorption due to H-bonded methanol OH groups (3600–3100 cm^{-1}) is clearly noted. This $\nu_{O–H\cdots O}$ stretching band sharpening and the passage, in the early stages of methanol uptake, of the apparent band maximum from ∼3450 to ∼3320 cm^{-1} corresponds to the passage of the early physisorption process from the preferable uptake of the first (few) methanol molecules by the formation of 2–3 distorted H-bondings ($\Delta\nu_{OH} \approx -300\,cm^{-1}$) to the formation of single virtually non-distorted H-bondings ($\Delta\nu_{OH} \approx -430\,cm^{-1}$), in which the O–H···O angle is close to 180° [19].
3. The overall intensity of the spectral patterns relative to the thin sample of the high-area A_{300} system (spectral sets a and c in Fig. 5B) is definitely larger than that of the corresponding low-area A_{50} system (spectral sets a and c in Fig. 5A), though not quite as much as one would expect on the basis of a surface area ratio close to ≈6:1 existing between the two Aerosil preparations. At the same time, we observe that the overall intensity of the spectral patterns of the thick $A_{50}300$ and $A_{300}300$ systems (spectral set d in Fig. 5A and B) is larger than that of the corresponding thin samples (spectral sets a in Fig. 5A and B), though not as much as one would expect on the basis of a sample weight ratio close to ≈5:1 or ≈6:1 existing between samples of different "thickness" of the same Aerosil preparations.

There is thus an apparent mismatch between the quantitative expectations imposed by the volumetric isotherms of Fig. 4, and the intensities of the adsorption spectral patterns reported in Fig. 5. In order to check this apparent mismatch in real quantitative terms, we have tried to build optical adsorption isotherms for methanol physically adsorbed by H-bonding, as well as for chemisorbed methanol, on the various Aerosil samples considered. As indicated in Section 1, the comparison between volumetric and optical adsorption isotherms should lead us, by the use of Eq. (6), to the evaluation of apparent molar absorption coefficients for the two types of adsorbed methanol species. The obtainment of constant (or non-constant) values for the coefficients in all experiments examined should so indicate us if equations of the B–L type do (or do not) actually apply to the adsorption processes here considered.

As analytical bands for adsorbed methanol we have considered the envelope of CH_3 stretching modes in the 3100–2700 cm^{-1} interval (examples of which were shown in Fig. 3), integrated after being accurately "cleaned", by band subtraction, of all contributions deriving from:

- superposition with the long low-ν tail of the broad band due to H-bonded OH;
- CH_n contributions from contaminants, possibly present in the starting background spectra (e.g., see spectrum a in the spectral set of Fig. 3A, and the lowest spectrum in the spectral patterns a and d in Fig. 5A and B, relative to $A_{50}300$ and $A_{300}300$, respectively);
- contributions from a chemisorbed methanol phase that was possibly formed during the build-up of the primary adsorption runs (e.g., see spectra b–d in the spectral set of Fig. 3B, relative to $A_{300}1073$), or was possibly present during the build-up of the secondary adsorption runs (e.g., see the lowest spectrum in the spectral pattern c of Fig. 5, relative to both $A_{50}1073$ and $A_{300}1073$).

Note that, besides ν_{CH} modes, other IR bands pertinent to the adsorbed methanol phases could in principle be used as analytical ones. For instance, we tried to use also the CH_3 deformation modes located in the 1550–1280 cm^{-1} spectral range, where the effects due to light scattering are expected to be lower. The results we obtained in terms of apparent extinction

coefficients were either comparable to those obtained in the ν_{CH} modes range, or (most frequently) poorer, due to far heavier difficulties in subtracting from experimental overall spectral absorptions the steep silica background and the overlapping contribution(s) due to vibrations involving surface OH species.

Using the cleaned CH_3 stretching bands obtained in the 3100–2700 cm^{-1} interval, optical secondary adsorption isotherms were so obtained, and are reported (together with one primary adsorption isotherm) in the first two parts of Fig. 6 (normalized absorbance units vs. methanol pressure). As for the chemisorbed methanol phase, the non-equilibrium isotherms for $p < 70$ Torr are reported, whereas for $p = 70$ Torr is reported the normalized absorbance figure obtained after the prolonged contact with methanol vapour followed by prolonged evacuation (i.e., the amount corresponding to the equilibrium saturation of all chemisorptive activity). Finally, the third part of Fig. 6 reports, for both A_{50} and A_{300}, one of the secondary adsorption isotherms and one saturation chemisorption datum obtained with thick samples.

Already after a first superficial inspection of the optical adsorption data reported in Fig. 6, it can be inferred that, from the quantitative point of view, the results are not really encouraging, and do not allow to expect the obtainment of constant absorption coefficients by comparison between optical and volumetric isotherms. In particular, it is immediately evident that the overall shape of the optical adsorption isotherms is quite different for the A_{50} systems of Fig. 6A (low surface area, large particles, high light scattering) and for the A_{300} systems of Fig. 6B (high surface area, small particles, low light scattering).

Entering into some detail, the following can be noted:

1. The optical adsorption isotherms of Fig. 6A, relative to $A_{50}T$ systems, do confirm that, on increasing the activation temperature, the adsorbing capacity towards methanol decreases, but the decrease of the optical response is far less pronounced than that previously observed and discussed on the basis of the volumetric isotherms of Fig. 4A. It is known that on varying the activation temperature (i.e., the degree of surface dehydration) of a dispersed solid, the dielectric properties of the interface change, and this change seems to affect to an appreciable extent

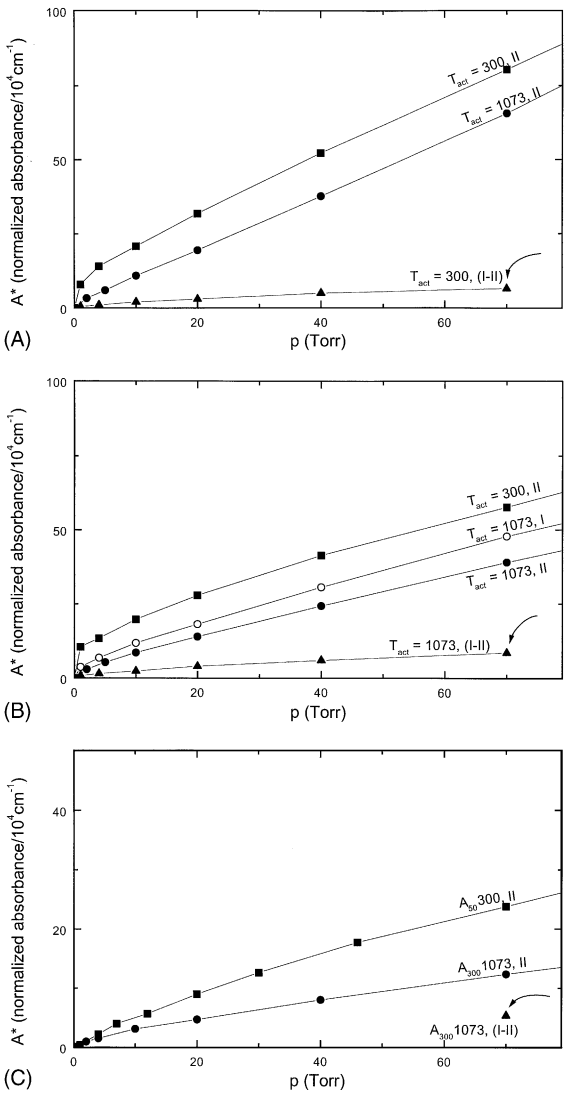

Fig. 6. Normalized optical adsorption isotherms (integral absorbance units vs. Torr) of methanol adsorbed at ∼300 K on thin Aerosil samples $A_{50}T$ (A), on thin Aerosil samples $A_{300}T$ (B), and on thick Aerosil samples of both $A_{50}T$ and $A_{300}T$ (C). The sample activation conditions are reported on the curves. The symbols I and II stand for primary and secondary adsorption run, respectively. The lower-lying curves, marked (I − II) in (A) and (B), correspond to the irreversibly adsorbed (chemisorbed) methanol phase. The experimental points reported on the optical chemisorption isotherms for $p < 70$ Torr do not represent equilibrium conditions, whereas the last chemisorption points, reported at $p = 70$ Torr in all parts and indicated by an arrow, are equilibrium points (i.e., obtained after prolonged contact with the highest methanol pressure) and represent the saturation chemisorptive capacity for each sample activated at high temperature.

the surface optical features of a compacted powdery system or, at least, those of a highly scattering system like A_{50}. As a consequence, a higher adsorbing capacity per surface OH group is simulated for the $A_{50}1073$ system, and this should lead to an absorption coefficient for physisorbed methanol that is not constant, but increases with increasing activation temperature.

An even more important aspect of the two top curves in Fig. 6A is that for both $A_{50}300$ and $A_{50}1073$, the (secondary) optical adsorption isotherms *do not* run parallel to the corresponding volumetric ones (see the curves marked $T_{act} = 300$ (II), and $T_{act} = 1073$ (II) in Fig. 4A). The optical uptake starts quite low, especially for the sample activated at high temperature, and keeps growing very steeply in the whole methanol pressure range explored, whereas the volumetric uptake starts quite high (as typical of type II isotherms in the BDDT classification [31]), and then knows a relatively moderate increase for pressures up to some 60–70 Torr. In other words, the trend with coverage of IR spectral data indicates a fast increasing adsorbing capacity that is not to be found in the "real" quantitative adsorption trend. This artefact is very difficult to interpret. Still, on the basis of the comparison with the behaviour exhibited by the $A_{300}T$ systems (to be dealt below) as well as of other similar adsorbing systems, the artefact is thought to be related to the highly scattering nature of the low-area A_{50} system. This physical property, peculiar of A_{50} systems, is bound to bring about a large and coverage-dependent difference between the two *d* terms in Eq. (2) (i.e., between the geometrical and the optical thickness of the adsorbing sample), and would so render the simplifying passage from Eq. (2) to Eq. (3) largely arbitrary.

In order to check in quantitative terms the limits of reliability of the comparison between optical and volumetric data, the isotherms have been "sampled" at three methanol equilibrium pressures (namely: 20, 40, and 60 Torr, respectively), and apparent molar absorption coefficients have been so calculated. For the $A_{50}T$ system, the ε_{CH_3} figures obtained are reported in the first part of Table 1 (see the rows marked 300 (II) and 1073 (II), columns 3, 5, and 7, relative to thin A_{50} samples).

As expected on the basis of what observed above, it is found that the apparent molar extinction coefficient of physisorbed methanol keeps growing with pressure in each isotherm (between 20 and 60 Torr, the increase is of some 20–35%), and also grows on passing from low-temperature to high-temperature specimens (the increase is of the order of some 50%).

It is so quite evident that, in these conditions, the concept of molar absorption coefficient does not apply, and the IR spectroscopic datum of physisorbed methanol possesses very little quantitative meaning, if any.

2. In the case of the high-area and low-scattering $A_{300}T$ systems (Fig. 6B), optical isotherms run much more parallel to the corresponding volumetric ones (see Fig. 4B), and also the decrease

Table 1
Apparent molar absorption coefficients for methanol adsorbed, at different adsorptive pressures, on some Aerosil samples ($mol^{-1}\ cm \times 10^{-6}$)

	20 Torr CH_3OH		40 Torr CH_3OH		60 Torr CH_3OH	
A_{50}	36 mg cm^{-2}	7 mg cm^{-2}	36 mg cm^{-2}	7 mg cm^{-2}	36 mg cm^{-2}	7 mg cm^{-2}
300 (II)	1.7	6.3	2.3	7.7	2.6	8.3
1073 (II)		9.2		10.6		11.0
1073 (irr)						Eq.: 3.6
A_{300}	39 mg cm^{-2}	6.5 mg cm^{-2}	39 mg cm^{-2}	6.5 mg cm^{-2}	39 mg cm^{-2}	6.5 mg cm^{-2}
300 (II)		5.5		5.8		5.9
1073 (II)	1.7	5.1	1.7	5.3	1.8	5.4
1073 (irr)					Eq.: 4.8	Eq.: 8.5

The symbol (II) stands for "secondary physisorption isotherm"; the symbol (irr) stands for "irreversible methanol phase" (or "chemisorbed methanol"); the symbol Eq. stands for "after equilibration with methanol vapour and prolonged evacuation at ambient temperature".

of the adsorbing capacity on passing from the low-temperature sample to the high-temperature sample seems more realistic. The calculation of apparent molar absorption coefficients at the usual three equilibrium pressures yields the figures reported in the second part of Table 1 (rows marked 300 (II) and 1073 (II), columns 3, 5, and 7, relative to thin $A_{300}T$ samples): ε_{CH_3} values fairly constant around 5.5×10^6 cm mol^{-1} are obtained, both within the same isotherm (on increasing the methanol pressure there is still a moderate increase of the apparent absorption coefficient, but nothing to compare with that observed with the A_{50} system), and in different isotherms (i.e., for different activation temperatures). This implies that, in a very low scattering system (as was monitored by Fig. 2 to be the case for the A_{300} system), the assumption of equivalence between optical and geometrical thickness is a reasonable one, and also the change of surface polarity brought about by the high temperature activation does not modify to an appreciable extent the surface optical features in the mid-IR range.

The behaviour of a similar low-scattering Aerosil system (the system $A_{200}T$, that is also non-porous and whose surface area is 205 m^2 g^{-1}) was found to be very similar to that of A_{300}. These observations imply that the concept of apparent molar extinction coefficient is probably usable, when the adsorption on low scattering systems is dealt with, at least as far as the constancy of the specific absorption is concerned. In fact, the *absolute* values of the coefficients ε_{CH_3} have not been checked yet (and will be checked in a following section), but the linearity of the optical response to the physical adsorption phenomenon is, in this case, confirmed.

3. The lower-lying curves in Fig. 6A and B (optical isotherms) and Fig. 4A and B (volumetric isotherms) correspond to the fraction of methanol that remains irreversibly adsorbed on the two Aerosil samples activated at high temperature. All points were obtained by difference between primary and secondary adsorption isotherms and correspond, especially in the case of the fast-collected spectroscopic data, to non-equilibrium conditions (in that methanol chemisorption depends on contact time as well as on pressure). The only exception is represented by the last point of each chemisorption curve, as these points were obtained after a long contact with the largest methanol dose, and thus correspond to equilibrium conditions. It is quite evident that the optical chemisorption data *do not* parallel the volumetric chemisorption data, as the latter ones indicated for $A_{50}1073$ a chemisorptive capacity approximately twice as large as that of $A_{300}1073$ (at equilibrium, ∼2 vs. ∼1.1 μmol m^{-2}, or ∼1.2 vs. ∼0.65 methoxyl groups nm^{-2}), whereas on the basis of the spectral data of Fig. 6 the chemisorptive capacity of $A_{300}1073$ turns out to be larger than that of $A_{50}1073$.

If the last (equilibrium) optical data of methanol chemisorption (marked by the arrows in Fig. 6) are compared with the corresponding volumetric data (marked with the arrows at $p = 70$ Torr in Fig. 4), the apparent extinction coefficients reported in Table 1 are obtained (see the rows marked 1073 (irr), column 7): the calculated coefficient ε_{CH_3} for chemisorbed methanol turns out to be $\sim 3.6 \times 10^6$ mol^{-1} cm for $A_{50}1073$, whereas it is $\sim 8.5 \times 10^6$ mol^{-1} cm for $A_{300}1073$.

It is quite difficult to propose a valid explanation for this large difference, because so far we have collected only a few data and several physical properties may be so different in the two silica specimens as to justify the peculiar experimental behaviour. Still, the simplest possibility that one can think of is that, unlike the much more abundant multilayer physical adsorption dealt with above, the chemisorption process (that is eminently localized, and involves only a fraction of the *first* adsorbed layer) leads to a spectroscopic response that depends to a large extent on the specific surface area of the adsorbing material. In other words, for a chemisorbed phase, the dependence of the spectral response on surface area would not be a linear one and, therefore, the surface area normalization introduced in Eq. (4) does not lead to constant values for the apparent absorption coefficient. An indirect (and quite weak) confirmation to this hypothesis comes, once more, from the system $A_{200}1073$, that is not presented here in much detail: in the case of this high-area adsorbent, the apparent absorption coefficient of chemisorbed methanol turns out to be $\sim 5.5 \times 10^6$ mol^{-1} cm, i.e., a figure somewhat intermediate between the figures obtained for the

higher-area and the lower-area systems of the same Aerosil family.

In any event, no matter what the ultimate explanation might be for the variable value of ε_{CH_3} for chemisorbed methanol, it is quite evident that, also in the case of methanol chemisorbed on Aerosil systems activated at high temperature, the concept of molar absorption coefficient is virtually impossible to apply in general terms.

4. The heaviest failure of the possibility of using with confidence the concept of molar absorption coefficients when dealing with heterogeneous surface processes (i.e., the existence of constant and reproducible specific absorbencies for adsorbed species) is contained in the data shown in Fig. 6C. The figure reports two secondary adsorption isotherms and one equilibrium chemisorption datum relative to thick samples, i.e., samples whose surface density (mg cm^{-2}) was kept deliberately much larger than in the case of the thin samples dealt with so far. The top curve of Fig. 6C is relative to methanol uptake on $A_{50}300$, whereas the lower curve and the equilibrium chemisorption datum therewith are relative to methanol uptake on $A_{300}1073$. By comparison of these optical adsorption data with the corresponding quantitative adsorption data of Fig. 4, the apparent absorption coefficients reported in Table 1 (columns 2, 4, and 6) are obtained. The data of Fig. 6C and the relevant coefficients reported in Table 1 confirm that, with highly scattering systems like A_{50}, the optical response to the adsorption process is unexpectedly steep and does not parallel the shape of the corresponding volumetric adsorption isotherm, whereas in the case of little scattering systems like A_{300} optical and volumetric isotherms run parallel and reasonably constant absorption coefficients are obtained. But the most important aspect evidenced by the data of Fig. 6C is that, by using thicker samples, much lower absorption coefficients are obtained than in the case of thin samples of the same adsorbing systems. This is the consequence of the fact that the optical response of a given adsorbed species (in the present case, the stretching modes envelope of the CH_3 groups) varies with the amount of the adsorbent in a non-linear way, so that the weight normalization introduced in Eq. (4) does not work. Also the equilibrium methanol chemisorption datum reported in Fig. 6C for $A_{300}1073$ (and marked with the arrow) indicates that the observed band intensities do not vary linearly with the sample surface density so that, the heavier the sample, the lower are the calculated absorption coefficients.

This latter observation, relative to the relationship between sample weight and IR bands intensity in adsorption processes, definitely rules out the possibility of using with confidence equations of the B–L type in surface chemistry, and the possibility of transferring calculated apparent absorption coefficients from one system to another one, though of the same chemical and/or physical type.

3.4. The molar absorption coefficients of methanol in homogeneous phase

The last aspect that has been considered concerns the *absolute* values of the apparent molar absorption coefficients obtained for both physisorbed and chemisorbed methanol on Aerosil, and reported in Table 1. The question we wanted to answer is: apart from the variability of the absorption coefficients and the various reasons that determine their variability, are the calculated absorption coefficients of adsorbed methanol of the right order of magnitude? We have therefore calculated the integral molar absorption coefficient of the same envelope of CH_3 stretching modes in the case of methanol dissolved in CCl_4 (a typical non-associating solvent, that only allows H-bondings of the solute–solute type) and in $CHCl_3$ (a typical associating solvent, that allows H-bondings of both solute–solvent and solute–solute type). Numerous solutions in the range 0.1–1.0 M were examined and, needless to say, in both cases perfectly linear B–L plots (i.e., absorbance vs. concentration plots) were obtained. The integral absorption coefficients obtained were: $5.2 \pm 0.4 \times 10^6$ mol^{-1} cm in the case of $CHCl_3$ solutions, and $7.0 \pm 0.5 \times 10^6$ mol^{-1} cm in the case of CCl_4 solutions.

These figures indicate that: (i) the molar absorption coefficient of the CH_3 stretching modes varies somewhat, in homogeneous phase, on varying the solvent and thus the conditions of H-bonding formation, but the changes are quite small, as expected of scarcely "sensitive" groups like saturated CH_n groups [32]; (ii) the apparent molar absorption coefficients calculated

for both physisorbed and chemisorbed methanol, and reported in Table 1, are indeed of the right order of magnitude, but the actual values vary under the effect of several variables much more than is acceptable for a scarcely sensitive group like OCH_3.

4. Conclusions

The use of Aerosil preparations as adsorbents has revealed as very convenient in order to test the possibility of using equations of the B–L type in adsorption phenomena, because Aerosil preparations allow to compare the behaviour of adsorbents of the same chemical type, but with fairly different physical characteristics. In other words, the use of Aerosil allowed us to compare the quantitative aspects of adsorption phenomena in virtually "extremely-different" conditions. No other oxidic adsorbents could be so easily tested by varying of almost one order of magnitude either the specific surface area of the adsorbent or the sample surface density, without varying the preparative conditions.

Also the use of methanol as adsorptive has revealed as quite convenient, because this test molecule allows to compare simultaneous physisorption and chemisorption phenomena, and allows to test the physisorption process in conditions in which the physisorptive uptake occurs to very different extents (by simply varying the adsorbent's activation conditions).

If adsorption processes are tested in quantitative terms in such extremely-different conditions, the conclusions that can be drawn on the possibility of using equations of the B–L type for heterogeneous systems (conclusions that have been already largely presented in Section 3) are as follows:

1. The assumptions that adsorption phenomena occur "homogeneously" in the whole adsorbing sample, and that the geometrical and optical thickness of the adsorbing sample are virtually equivalent are basically wrong. The deviation with respect to the ideal, "homogeneous" behaviour is larger, the heavier are the light-scattering characteristics of the adsorbent.
2. The IR spectroscopic response to adsorption phenomena is largely non-linear with respect to some important physical parameters like, for instance, specific surface area and sample weight. As a consequence, all types of optical data normalization that one can try to introduce in order to render comparable results deriving from different experiments are, in general terms, wrong. To be less drastic, we may suppose that optical data normalization procedures are probably adequate if they try to compensate only (very) minor differences of either surface area or sample surface density.

A last conclusive comment concerns the cases (actually, very few) in which the use of and comparison between molar absorption coefficients for adsorbed species seemed to work reasonably well: it is quite likely that, without knowing or thinking of it, systems and/or samples of comparable scattering features, comparable surface area, and comparable sample weight were actually used. This is certainly the case with, for instance, our numerous works devoted in the past 10 years or so to the weak, scarce and reversible room temperature adsorption of CO on metal oxides of the fourth group.

Acknowledgements

This work was partly financed by Italian MURST (Rome), Cofin 98, Section 03.

References

[1] J. Oscik, Adsorption, Ellis Horwood Series in Physical Chemistry, Wiley, New York, 1982, p. 27 (Chapter 3).
[2] C. Morterra, E. Garrone, V. Bolis, B. Fubini, Spectrochim. Acta A 43 (1987) 1577.
[3] V. Bolis, B. Fubini, E. Garrone, C. Morterra, J. Chem. Soc., Faraday Trans. I 85 (1989) 1383.
[4] E. Garrone, V. Bolis, B. Fubini, C. Morterra, Langmuir 5 (1989) 892.
[5] V. Bolis, C. Morterra, M. Volante, L. Orio, B. Fubini, Langmuir 6 (1990) 695.
[6] T.R. Hughes, H.M. White, J. Phys. Chem. 71 (1967) 2192.
[7] C.A. Emeis, J. Catal. 141 (1993) 347.
[8] T. Barzetti, E. Selli, D. Moscotti, L. Forni, J. Chem. Soc., Faraday Trans. 92 (1996) 1401.
[9] S. Khabtou, T. Chevreau, J.-C. Lavalley, Micropor. Mater. 3 (1994) 133.
[10] V. Bolis, G. Cerrato, G. Magnacca, C. Morterra, Thermochim. Acta 312 (1998) 63.
[11] E. Borello, A. Zecchina, C. Morterra, J. Phys. Chem. 71 (1967) 2938.
[12] E. Borello, A. Zecchina, C. Morterra, G. Ghiotti, J. Phys. Chem. 71 (1967) 2945.

[13] C. Morterra, M.J.D. Low, J. Phys. Chem. 73 (1969) 321.
[14] A.V. Kiselev, V.I. Lygin, K.L. Schepalin, Kinet. Catal. 12 (1971) 154.
[15] N. Takezawa, H. Kobayashi, J. Catal. 25 (1972) 179.
[16] G. Mertens, J.J. Fripiat, J. Colloid. Interf. Sci. 42 (1973) 169.
[17] B.A. Morrow, J. Chem. Soc., Faraday Trans. I 70 (1974) 1527.
[18] B.A. Morrow, J. Phys. Chem. 81 (1977) 2663.
[19] A.G. Pelmenschikov, A.G. Morosi, A. Gamba, J. Phys. Chem. 96 (1992) 2241.
[20] A.G. Pelmenschikov, A.G. Morosi, A. Gamba, A. Zecchina, S. Bordiga, E.A. Paukshtis, J. Phys. Chem. 97 (1993) 11979.
[21] A.G. Pelmenschikov, A.G. Morosi, A. Gamba, J. Phys. Chem. 101 (1997) 1178.
[22] M.A. Natal-Santiago, J.A. Dumesic, J. Catal. 175 (1998) 252.
[23] B.A. Morrow, I.A. Cody, J. Phys. Chem. 80 (1976) 1995.
[24] B.A. Morrow, I.A. Cody, J. Phys. Chem. 80 (1976) 1998.
[25] B.A. Morrow, I.A. Cody, J. Phys. Chem. 80 (1976) 2761.
[26] P. Hoffmann, E. Knözinger, Surf. Sci. 188 (1987) 181.
[27] B. Fubini, V. Bolis, A. Cavenago, E. Garrone, P. Ugliengo, Langmuir 9 (1993) 2712.
[28] J. Cortes, M. Jensen, P. Araya, J. Chem. Soc., Faraday Trans. I 82 (1986) 1351.
[29] B.A. Morrow, I.A. Cody, J. Phys. Chem. 77 (1973) 1465.
[30] B. Onida, M. Allian, E. Borello, P. Ugliengo, E. Garrone, Langmuir 13 (1997) 5107.
[31] S. Brunauer, L.S. Deming, W.S. Deming, E. Teller, J. Am. Chem. Soc. 62 (1940) 1723.
[32] N.B. Colthup, L.H. Daly, S.E. Wiberley, Introduction to Infrared and Raman Spectroscopy, Academic Press, New York, 1975, p. 223.
[33] V. Bolis, B. Fubini, E. Garrone, C. Morterra, P. Ugliengo, J. Chem. Soc., Faraday Trans. 88 (1992) 391.
[34] V. Bolis, C. Morterra, B. Fubini, P. Ugliengo, E. Garrone, Langmuir 9 (1993) 349.
[35] V. Bolis, A. Cavenago, B. Fubini, Langmuir 13 (1997) 895.